Title

110th Anniversary: Theory of Activity Coefficients for Lithium Salts in Aqueous and Nonaqueous Solvents and in Solvent Mixtures

Journal

Industrial and Engineering Chemistry Research, 58(39)

ISSN

0888-5885

Authors

Crothers, AR
Radke, CJ
Prausnitz, JM

Publication Date

2019-10-02

DOI

10.1021/acs.iecr.9b02657

Peer reviewed

110th Anniversary: Theory of Activity Coefficients for Lithium Salts in Aqueous and Nonaqueous Solvents and in Solvent Mixtures

Andrew R. Crothers, Clayton J. Radke, and John M. Prausnitz*

Department of Chemical and Biomolecular Engineering, University of California, Berkeley, California 94720-1462, United States

Corresponding Author *E-mail: prausni@berkeley.edu.

Abstract

On the basis of work by Bernard and Blum [Bernard, O.; Blum, L. Binding Mean Spherical Approximation for Pairing Ions: An Exponential Approximation and Thermodynamics. J. Chem. Phys. 1996, 104, 4746–4754], Barthel et al. [Barthel, J.; Krienke, H.; Holovko, M.; Kapko, V.; Protsykevich, I. The Application of the Associative Mean Spherical Approximation in the Theory of Nonaqueous Electrolyte Solutions. Condens. Matter Phys.2000, 3, 23], and Simonin et al. [Simonin, J.-P.; Bernard, O.; Blum, L. Real Ionic Solutions in the Mean Spherical Approximation. 3. Osmotic and Activity Coefficients for Associating Electrolytes in the Primitive Model. J. Phys. Chem. B1998, 102, 4411–4417], this work presents and validates a molecular-thermodynamic model for lithium salt activity coefficients in aqueous and nonaqueous single- and mixed-solvent systems. The Binding Mean Spherical Approximation gives electrolyte activity due to long-range electrostatic forces, short-range hard-sphere repulsion, and ion-pair formation. The theory shows good agreement with measured salt activities up to 3 molar in aqueous and nonaqueous solvents using a solvent-dependent, concentration-independent, center-to-center distance of closest approach between ions as the single fitting parameter for each electrolyte system. For mixed-solvent electrolytes, the local solvation environment around the ions dictates short-range interactions. To account for preferential ion solvation in a mixed solvent, the center-to-center distance is obtained from Wang and co-workers’ Dipolar Self-Consistent-Field Theory [Nakamura, I.; Shi, A.-C.; Wang, Z.-G. Ion Solvation in Liquid Mixtures: Effects of Solvent Reorganization. Phys. Rev. Lett. 2012, 109, 257802]. For a particular salt in a binary solvent mixture at fixed temperature, the model predicts salt activity coefficients using only the fitted single-solvent distances-of-closest approach.

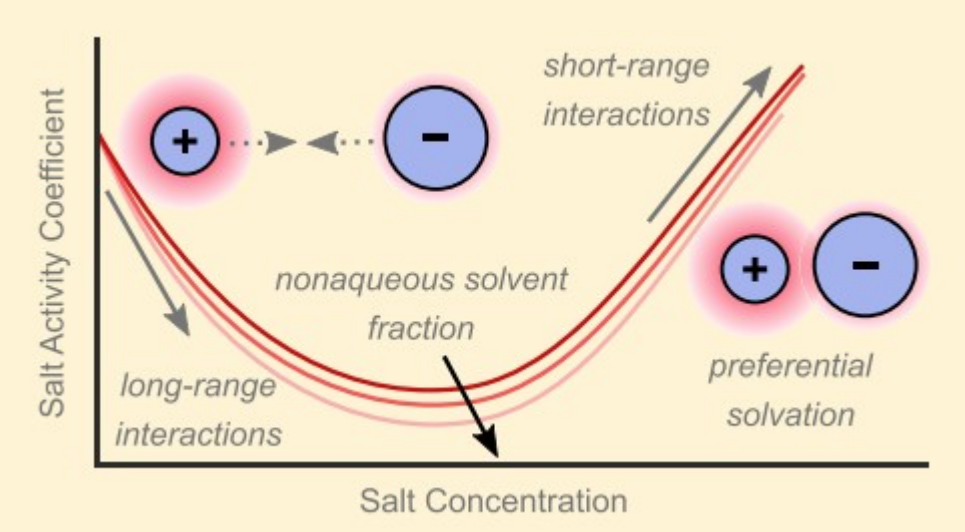

Introduction

Sustainable electrochemical technologies, such as lithium-ion batteries, frequently use nonaqueous or mixed-solvent electrolytes.(1−3) Depending on the application, solvent mixtures may be water–alcohol, as in electrochemical reduction of CO_2 to alcohols,(4) or nonaqueous mixtures, such as two aprotic solvents (*e.g.*, two carbonates) in lithium-ion batteries.(5) The performance of electrochemical systems is influenced by the thermodynamic properties of the electrolyte.(6)

The literature is rich on the properties of electrolyte solutions; however, most of that literature concerns aqueous systems.(7,8) Much less attention has been given to nonaqueous systems.(5,9−15) Published equations for salt activity coefficients are based on essentially empirical extensions of the Debye–Hückel theory to high salt concentrations.(16) In particular, Pitzer's(17) equation is a very popular approach to calculate salt activity coefficients in concentrated electrolytes. However, many of these models require numerous adjustable parameters. Several authors have experimentally characterized the thermodynamic activities of mixed-solvent electrolytes and a few microscale models have been presented based on pertinent molecular interactions.(10,12,18,19)

In solvent mixtures, experimental and theoretical research has long ago shown that polarizable solvents and those with strong specific interactions preferentially solvate ions.(20−22) As a result of preferential solvation, activity coefficients of salts in a solvent mixture are not simple averages of pertinent single-solvent electrolyte properties.(12,19,23−28) Authors often interpolate properties from those of single-solvent electrolytes using arbitrary mixing rules or equations with multiple adjustable parameters.(12,19,23−28)

A promising method to gain tractable expressions for salt activity coefficients in electrolytes is based on the McMillan–Mayer framework(29) that considers

the solvent to be a continuous dielectric medium. In this framework, integral-solution theory calculates activity coefficients for electrolytes in solution.(29,30) Electrostatic interactions between ions occur over length scales corresponding to many solvent-molecule diameters (i.e., long-range), whereas hard-sphere repulsive effects lead to interactions that occur over a distance of one or two solvent diameters (i.e., short-range).(29) Long-range electrostatic forces depend on the dielectric constant of the solvent; short-range interactions depend on the diameters of the solvated ions. In a mixed solvent, due to preferential solvation, the composition of the solvent in the bulk is not the same as that at the ion surface.

Here we apply the mean spherical approximation (MSA)(31) integral-solution theory modified by taking ion-pairing into account. That theory, pioneered by Bernard and Blum,(32) Simonin et al.,(33) and Barthel et al.,(9) is called the binding MSA (BiMSA). Because the dielectric constant of a typical nonaqueous solvent is well below that of water, ion-pair formation in nonaqueous solvents is more extensive than in water. A major advantage of BiMSA is that for practical results, BiMSA requires only the solvated diameter of each ion as an adjustable parameter. To determine an effective ion diameter in a solvent mixture, we use results from Wang and co-workers who presented a dipolar self-consistent-field theory (DSCFT) that relates the bulk solvent composition to that of the local solvent environment around a solvated ion.(21,22)

We first summarize pertinent thermodynamic variables. Next, we briefly review the MSA theory for electrolyte solutions. We then discuss the BiMSA extension of that theory to take ion-pair formation into account. We then show predictions for aqueous and nonaqueous single-solvent electrolyte solutions. Finally, we use DSCFT to calculate activity coefficients for salts in several mixed water–alcohol solvents using only the two solvated ionic diameters obtained from single-solvent data. Agreement with experiment is good.

Thermodynamic Background

Consider a system containing a solvent and a 1–1 salt A that consists of anion A^- and cation A^+:

$$A \rightarrow A^- + A^+ \quad (1)$$

A has molar concentration c. Assuming complete dissociation, anion and cation concentrations $c_- = c_+ = c$. Following thermodynamic convention, we define the chemical potential of a 1–1 salt as the sum of three parts: the reference chemical potential of A, the ideal mixing chemical potential of the fully dissociated electrolyte, and the excess chemical potential due to nonideality caused by ion–ion interactions including ion-pair formation(18)

$$\mu_A = \mu_A^\circ + 2RT \ln\left(\frac{c}{c^\circ}\right) + 2RT \ln(f_\pm) \quad (2)$$

where R is the gas constant and T is the temperature. The first term on the right side of eq 2, μ_A^θ, is the reference chemical potential of salt A in a hypothetical, ideal, fully dissociated solution of salt concentration c^θ in the same solvent and at the same temperature and pressure as those of the system. When concentration is molarity, c^θ is equal to unit molarity; superscript θ indicates the reference (standard) state. The second term in eq 2 comes from the hypothetical ideal mixing of the fully dissociated ions in the solvent where the factor 2 comes from salt A dissociating into two ions.(6) The dimensionless mean molar activity coefficient of the salt $f_\pm$ accounts for the effect of interactions (e.g., excluded-volume repulsion, electrostatics, and ion association to ion pairs) not present in an ideal, fully dissociated solution. The activity coefficient $f_\pm$ is directly related to excess free energy. For an ideal solution, $f_\pm = 1$. Equation 2 is normalized, such that as $c \rightarrow 0$, $f_\pm \rightarrow 1$.(18) This statement is consistent with the electrolyte fully dissociating at infinite salt dilution.(18)

Frequently, the literature reports the mean molal activity coefficient $\gamma_\pm$. These two coefficients are related by(6)

$$f_\pm = \frac{d_s^0 \gamma_\pm}{c_s M_s} \quad (3)$$

where M_s is the solvent molar mass (or molar-averaged molar mass for a solvent mixture), c_s is the molar concentration of solvent (or a molar-averaged solvent concentration for a solvent mixture), and d_s^0 is the mass density of the salt-free solvent (or solvent mixture). Superscript 0 denotes salt-free; $\gamma_\pm$ and $f_\pm$ are dimensionless; subscript s stand for solvent. Typical units for the other quantities are d_s^0 (kg/dm^3); c_s (mol/dm^3); and M_s (kg/mol).

MSA Theory for $f_\pm$

For a 1–1 salt, the excess chemical potential of the salt μ_A^{ex} is related to $f_\pm$ by(34,35)

$$2RT \ln f_\pm = \mu_A^{ex} \quad (4)$$

The factor 2 in eq 4 comes from eq 2. μ_A^{ex} is given by(32,34,36)

$$n\mu_A^{ex} = F'^{ex} + VP^{ex} \quad (5)$$

where F'^{ex} is the excess modified Helmholtz free energy and P^{ex} is the excess pressure that arises from interionic interactions; the modified Helmholtz free energy F' is a thermodynamic potential that is a function of system volume V, temperature T, moles of salt n, and chemical potential of solvent μ_s [i.e., $F'(V, T, n, \mu_s)$].(34)F' is related to the unmodified Helmholtz free energy F, that is a function of solvent moles n_s rather than μ_s, through a Legendre transformation $F'(V, T, n, \mu_s) = F(V, T, n, \mu_s) - n_s\mu_s$.(34) Just as F is a Legendre transformation of internal energy E ($F = E - TS$), F' is a transformation of a modified internal energy $E' = E - n_s\mu_s = F' + TS$. As we show later, F' and E' are useful because they allow us to consider the solvent as an implicit

background medium as specified in the McMillan–Mayer framework. Various authors(34,35,37) note that μ_A^{ex} in eq 5 is the excess chemical potential of a system under an excess pressure P^{ex} that is not present during the measurement of $f_\pm$ and subsequent calculation of μ_A^{ex} using eq 4. The correction to eq 4 that makes it consistent with eq 5 is very small at low and moderate salt concentrations and is therefore neglected in this work.(34,35)

From standard thermodynamics,(32,34,36)

 (6)

The excess modified Helmholtz free energy is zero (i.e., solution is ideal) when the interaction energy of the ions is very small compared to k_BT where k_B is the Boltzmann constant. This condition is achieved as $T \to \infty$. We obtain F'^{ex} by integrating the excess modified internal energy E'^{ex} from $T = \infty$ to the system temperature T at constant V, n, and [illegible](32,36)

$$F'^{ex} = -T\int_{\infty}^{T} \frac{E'^{ex}}{T^2}\,dT \quad (7)$$

We determine E'^{ex} by summing over the integrated interactions between ions(32,36)

 (8)

where $\bar{\rho}_i$ is the bulk average number density of ion i in the solvent ($=c_iN_A$, where N_A is Avogadro's number) and $u_{ij}(r)$ and $g_{ij}(r)$ are the interionic potential function and radial distribution function between i and j at distance r. The radial distribution function $g_{ij}(r)$ is the number density of j, $\rho_j^{(i)}$, where j is a distance r from ion i normalized by $\bar{\rho}_j$ (*i.e.* $g_{ij}(r) = \rho_j^{(i)}(r)/\bar{\rho}_j$). Because we are using the McMillan–Mayer frame, the summations in eq 8 are over all ionic species i and j only; interaction with solvent molecules are not explicitly included.(32,36) Radial distribution function $g_{ij}(r)$ depends on salt concentration c and, to a lesser extent, on temperature T.

The positions of ions relative to one another, as described by g_{ij}, follow from interionic interactions between ions i and j. These interactions are described by c_{ij}, the direct correlation function. (Regrettably, letter c is commonly used both for concentration and for direct correlation function. The direct correlation function notation has two subscripts, c_{ij}, whereas concentration has no subscripts when referring to the salt concentration c, or one subscript when referring to solvent, c_s, or ion concentrations, c_+ and c_-.) The Ornstein–Zernike equation relates the position function (g_{ij}) and interaction function (c_{ij}) between ions i and j(36,38)

 (9)

where the integral is over all positions in space **r**. The first term on the right side of eq 9 gives the direct interactions between *i* and *j*; the second term gives the integrated interactions between *i* and *j* as caused by additional ions *k* summed over all *N* ionic species in the system. The purpose of the Ornstein–Zernike equation is to provide an expression that relates the radial distribution function to the solute density. In an ideal solution, g_{ij} is equal to 1 for all solute densities.(39)

Figure 1 shows an approximate schematic of the two parts of the Ornstein–Zernike equation. Fourier transformation methods solve eq 9 for g_{ij} (or c_{ij}) provided that we also specify an additional equation giving information about g_{ij} or c_{ij}(32,36) This additional equation is called the closure.

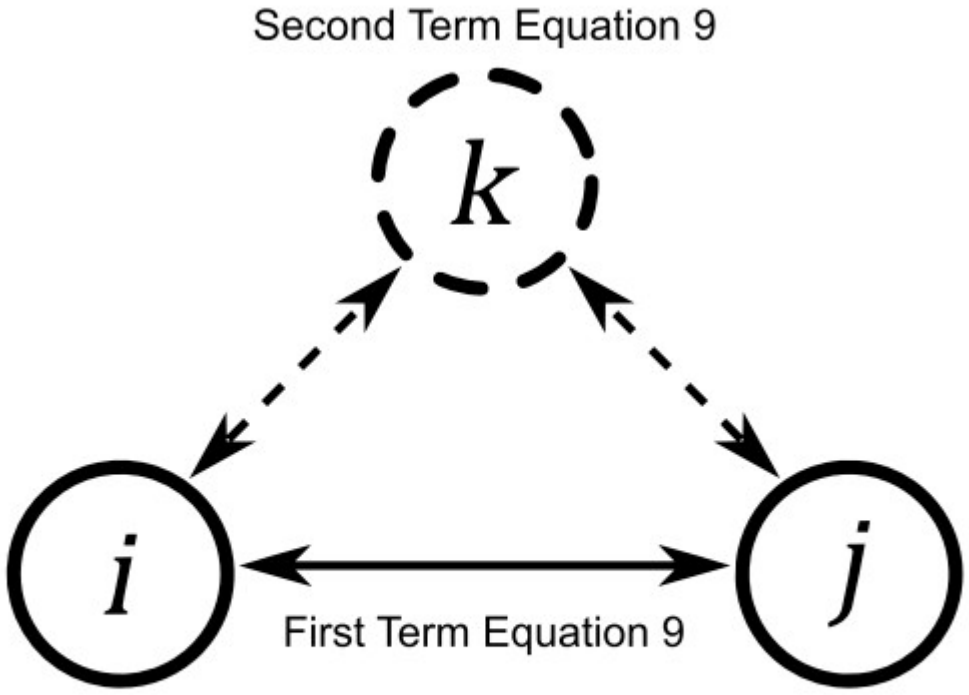

Figure 1. Illustration of the Ornstein−Zernike equation (eq 9) where the solid line is interactions as given by the first term and the dotted lines are indirect interactions given by the second term.

The MSA closure is a functional form for g_{ij} and c_{ij} that determines the electrostatic contribution to the excess modified energy E'^{el}. The MSA closure for eq 9 first specifies that(31,36)

$$g_{ij}(r) = 0, r < \sigma_{ij} \quad (10)$$

where σ_{ij} is the distance of closest approach between ions *i* and *j* (=(σ_i + σ_j)/2, where σ_i is the diameter of ionic species *i*). Equation 10 says that ion *j* cannot approach ion *i* closer than σ_{ij}; $\rho_j(r < \sigma_{ij}) = 0$. Second, MSA specifies

that for $r > \sigma_{ij}$, c_{ij} is proportional to u_{ij} where ions i and j interact via Coulombic electrostatic interactions(31,36)

 (11)

where ε_{vac} is vacuum permittivity, ε_r is the dielectric constant of the solvent, z_i is the valence of ion i, and e is the elementary charge. Although MSA theory does not give an analytical expression for $g_{ij}(r)$, the solution to eq 9 gives E'^{ex} by providing the term $\int_0^\infty u_{ij}(r)g_{ij}(r)4\pi r^2\,dr$ in eq 8. The tedious mathematical procedure is shown in ref (36). The radial distribution function $g_{ij}(r)$ is a function of ion concentration, ion size, ion charge, and system temperature.(36)

In conjunction with eqs 4–8, the MSA theory for $g_{ij}(r)$ gives an analytic solution to the electrostatic contribution to the activity coefficient $f_\pm^{el}$ for a 1–1 electrolyte in which the ions have equal diameters σ(36,40)

$$\ln f_\pm^{el} = -b\frac{\Gamma}{1+\Gamma\sigma} \quad (12)$$

where the superscript el denotes the electrostatic component of $f_\pm$. Γ is the MSA screening parameter

$$\Gamma = \frac{1}{2\sigma}[(1+2\sigma\kappa)^{1/2} - 1] \quad (13)$$

and b is the Bjerrum length

 (14)

κ is the Debye–Hückel screening parameter of the electrolyte

 (15)

where c is the molar concentration and N_A is Avogadro's number. The inverse of a screening parameter (1/κ) gives a characteristic distance (Debye length) where an ion is influenced by a central ion; in Debye–Hückel theory, κ is the screening parameter specified by eq 15 whereas the screening parameter Γ in MSA theory is specified by eq 13.(36)

Harvey et al.(41) showed that the linear average of two unequal ion diameters provides a very good approximation for salts whose ionic diameters are within a factor of 2. For a salt consisting of ions with arbitrarily unequal ionic diameters, Blum and Høye(31,40) showed that the MSA gives a set of algebraic equations that must be solved numerically to determine the mean ionic activity coefficient $f_\pm$.

Binding Mean Spherical Approximation for $f_\pm$

Hard-sphere interactions of the ions and ion pairing extend MSA to higher ionic concentrations.(32) The binding mean spherical approximation (BiMSA)

explicitly accounts for the interactions among free ions and ion pairs by using Wertheim's extension to the Ornstein–Zernike equation for associating species.(42) In addition to Coulombic long-range and hard-sphere short-range interactions, the BiMSA closure accounts for ion pairing.(32) Ion association is described by sticky-point attraction. The radial distribution function for unbound ions is approximated by that for the hard-sphere fluid influenced by electrostatic interactions.(32) Detailed derivations for activity coefficients based on BiMSA are given elsewhere.(9,32,43)

To obtain useful expressions, we give the ions a single effective diameter σ that is an average of the two solvated ion diameters; $\sigma = (\sigma_- + \sigma_+)/2$, where σ_- and σ_+ are the diameters of the solvated anion and cation. Here, we give the practical final form of the activity expressions for a 1−1 electrolyte. Reference (32) provides a detailed description of the generalized formulation that includes salts for which the diameter of the solvated cation is not equal to that of the solvated anion within a factor of 2.

The mean ionic activity coefficient is given by the sum of contributions from hard-sphere repulsion $f_{\pm}^{HS}$ that accounts for hard-body repulsions between ions and ion pairs; electrostatic $f_{\pm}^{el}$ that accounts for Coulombic interactions between ions; and for ion-pair formation $f_{\pm}^{IP}$ that accounts for association of free ions to form ion pairs

$$\ln f_{\pm} = \ln f_{\pm}^{HS} + \ln f_{\pm}^{el} + \ln f_{\pm}^{IP} \quad (16)$$

The Carnahan–Starling equation gives the hard-sphere contribution(32)

$$\ln f_{\pm}^{HS} = \frac{8\eta - 9\eta^2 + 3\eta^3}{(1-\eta)^3} \quad (17)$$

where η is a measure of ion concentration called the packing factor

$$\eta = \frac{\pi}{3} c N_A \sigma^3 \quad (18)$$

The hard-sphere contribution incorporates the impact of ion solvation on the free energy by including the volume excluded by the ions and their solvation shell; it is phenomenologically equivalent to the widely used Stokes-Robinson theory of solvation.(44)

The electrostatic contribution is(32)

$$\ln f_{\pm}^{el} = -b\frac{\Gamma_B}{1 + \Gamma_B \sigma} \quad (19)$$

where Γ_B is the BiMSA screening parameter. The form of eq 19 is the same as that of eq 12 with Γ replaced by Γ_B that accounts for ion-pairing. Γ_B is found by solution of the transcendental equation(31,32)

$$\eta(1 + \Gamma_B \sigma)^3 = \left(\frac{\kappa}{\Gamma_B}\right)^2 \frac{\delta + \Gamma_B \sigma}{1 + \Gamma_B \sigma} \quad (20)$$

where κ is given by eq 15 and δ is the fraction of all the ions that are not paired. Equilibrium between free and paired ions gives δ(32,45)

 (21)

where *K* is the dimensionless equilibrium constant. The term on the left side of eq 21 accounts for association equilibria of ideal unpaired cations and anions to ion pairs. The term in braces on the right side of eq 21 corrects the equilibria for nonidealities. The exponential term accounts for electrostatic interactions, and the term on the right side in brackets accounts for hard-sphere repulsions. For electrostatic association (ion-pairs) between spherical ions, (dispersion interactions are neglected because they are much smaller than electrostatic interactions), the equilibrium constant *K* is(45,46)

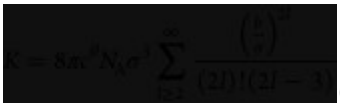 (22)

where *b* is given by eq 14. Given eq 21 and 22, the numerical solution to coupled eqs 20 and 21 provides δ and Γ_B; upon substitution into eq 19, we obtain $f_{\pm}^{el}$.

Ion-pairing affects salt activity through ln $f_{\pm}^{IP}$(32)

 (23)

where the first term on the right side accounts for the decreased fraction of free ions due to ion pairing and the second accounts for how ion pairing alters the hard-sphere contribution.

The only adjustable parameter is σ. The arithmetic average of the solvated ion diameters σ_- and σ_+ determines σ. To quantify the extent of cation solvation, we set σ_+ as the crystallographic diameter of the cation, σ_+^x (crystallographic is denoted with superscript x) plus a contribution from the solvent diameter σ_s

$$\sigma_+ = \sigma_+^x + 2\omega_s\sigma_s \quad (24)$$

where ω_s is a sphericity factor accounting for how the solvent molecules orient around the cation and how tightly they bind to the cation. For a spherical solvent molecule that tightly binds to the cation, $\omega_s = 1$, while $\omega_s = 0$ when the cation is not solvated. We set σ_- to the crystallographic diameter of the anion, σ_-^x, because anions tend to be larger and, therefore, more weakly solvated.(47) Upon adjusting σ for an electrolyte–solvent system to optimize agreement with experiment, eq 24 gives ω_s in terms of σ, σ_-^x, σ_+^x, and σ_s. ω_s is calculated from the fit σ for a given cation–anion pair in a given solvent; ω_s is independent of ion concentration and mixed-solvent composition. The Supporting Information provides a computer program for performing these calculations.

Comparison with Experiment

To establish how well the model fits experimental data, we use the average relative deviation (ARD) defined by

$$\mathrm{ARD} = \frac{1}{N_P} \sum_{c} \left| 1 - \frac{f_{\pm}^{\mathrm{calc}}(c)}{f_{\pm}^{\mathrm{exp}}(c)} \right| \quad (25)$$

where the sum over N_P salt concentrations c where experimental $f_{\pm}^{\mathrm{exp}}$ are available; $f_{\pm}^{\mathrm{calc}}$ is calculated from eq 16 at salt concentration c. Table1 provides physical constants for the solvents considered here.

Table 1. Properties of Solvents[a] at 298.15 K unless Otherwise Stated

solvent	M_s [kg mol^{-1}][48]	ε_r[48]	$D_s \times 10^{30}$ [m C][i49]	$v_s x 10^2$ [nm^{-3}][j48]	$\alpha_s \times 10^{40}$ [F m^2][m48]
water	0.018	78.4	6.17	3.00	1.61
1,4-dioxane	0.0881	2.21	1.50[d]	14.2	9.57
2-propanol	0.0601	19.3	5.54	12.7	8.47
acetone	0.0581	20.5	9.60	12.2	7.04
acetonitrile	0.0411	35.7	13.1	8.71	4.98
dimethyl carbonate	0.0901	3.09	3.00[e]	14.0[k]	8.57
ethanol	0.0461	24.9	5.64	9.69	5.69
ethyl methyl carbonate	0.104	2.99[b]	2.97[f]	17.1	10.5[d]
ethylene carbonate	0.0880	95.3[c]	16.2[g]	11.1[l]	7.34[h]
methanol	0.0320	32.6	5.67	6.73	3.66

[a] M_s is molecular mass, ε_r is dielectric constant, D_s is dipole moment, v_s is molecular volume, and α_s is polarizability. [b] Temperature = 293 K. [c] Reference 50. [d] Reference 29. [e] Temperature = 328 K. [f] Reference 51. [g] Reference 52. [h] Reference 53. [i] Frequently given in CGS units of Debye, D (1 D = 3.3356×10^{-30} m C where C is the unit coulomb). [j] Temperature = 293.15 K. Related to molar concentration by $v_s = \frac{1}{c_s N_A}$ where N_A is Avogadro's number and nm is the unit nanometer [k] Reference 54. [l] Temperature = 312 K. [m] Frequently given in CGS units of cm^3 (α_s [cm^3] = 8.988×10^{15} α_s [F m^2], where F is the unit farad).

Binding Mean Spherical Approximation for a Single-Solvent Electrolyte

Figure 2a shows measured and calculated (eq 16) mean ionic activity coefficients for $LiClO_4$ in water, methanol, ethanol, acetonitrile, acetone, and

2-propanol. Agreement between theory and experiment is good up to 2 molar for water, methanol, and ethanol (with ARDs 2.1%, 8.6%, and 6.1%, respectively) and excellent for 2-propanol, acetone, and acetonitrile (with ARDs 0.77%, 0.30%, 0.31%, respectively). (Fitting K to the experimental thermodynamic data slightly improves the fit for water and small alcohols, but introduces an additional adjustable parameter.) The results are consistent with those of Barthel and co-workers(9,45,55) and more recent work by Simonin and Bernard.(56) Using eq 24 and calculating σ_s from the solvent molecular volumes in Table1 ($\sigma_s = (6v_s)^{1/3}$), the fitting parameter σ gives ω_s that falls within the expected range of zero and 1. Table2 gives σ and ω_s for $LiClO_4$ in these solvents. Water and small alcohols have larger values of ω_s, indicating higher solvent sphericity or tighter solvent binding. For the other solvents, ω_s falls closely within a narrow range 0.19–0.21.

Table 2. Model Parameters for $LiClO_4$ at 298.15 K and Experimental Equilibrium Constant K^{lit}

solvent	σ [nm]	ω_s [a]	K [b]	K^{lit}
water	0.462	0.375	0.368	
methanol	0.655	0.668	9.07	
ethanol	0.624	0.536	30.3	43.1[57]
2-propanol	0.437	0.190	188	
acetone	0.448	0.211	129	132.3[58]
acetonitrile	0.422	0.190	10.7	17.1[59,60]

[a] Equation 24 where $\sigma^x_{Li^+} = 0.156$ nm, $\sigma^x_{ClO_4^-} = 0.480$ nm.[61,62] [b] Equation 22.

For all solvents, consistent with Debye–Hückel theory, the activity coefficients initially decrease with rising salt concentration because of favorable electrostatic interactions between ions, given by $\ln f_\pm^{el}$ from eq 19. (29) The dielectric constant of the solvent dictates how strongly the activity coefficient changes with salt concentration at high dilution. Ions in low dielectric-constant solvents associate more, as indicated in eq 22. At higher concentrations, ion–ion repulsion, given by $\ln f_\pm^{HS}$, create hard-sphere interactions that increase the activity coefficient. The ions' solvated hard-sphere size governs how activity coefficients increase with rising salt concentration. Our attribution of the upturn in $\ln f_\pm$ at high salt concentrations to the excluded volume of the ions and their solvation shell results from the solvation effects reported by other researchers.(8,12,44,63) With higher ion association there are fewer solute particles and, as eq 23 shows, association moderates the increase in activity coefficients by reducing repulsive interactions. This finding is consistent with previous research on activity coefficients of weak electrolytes.(39,43,64)

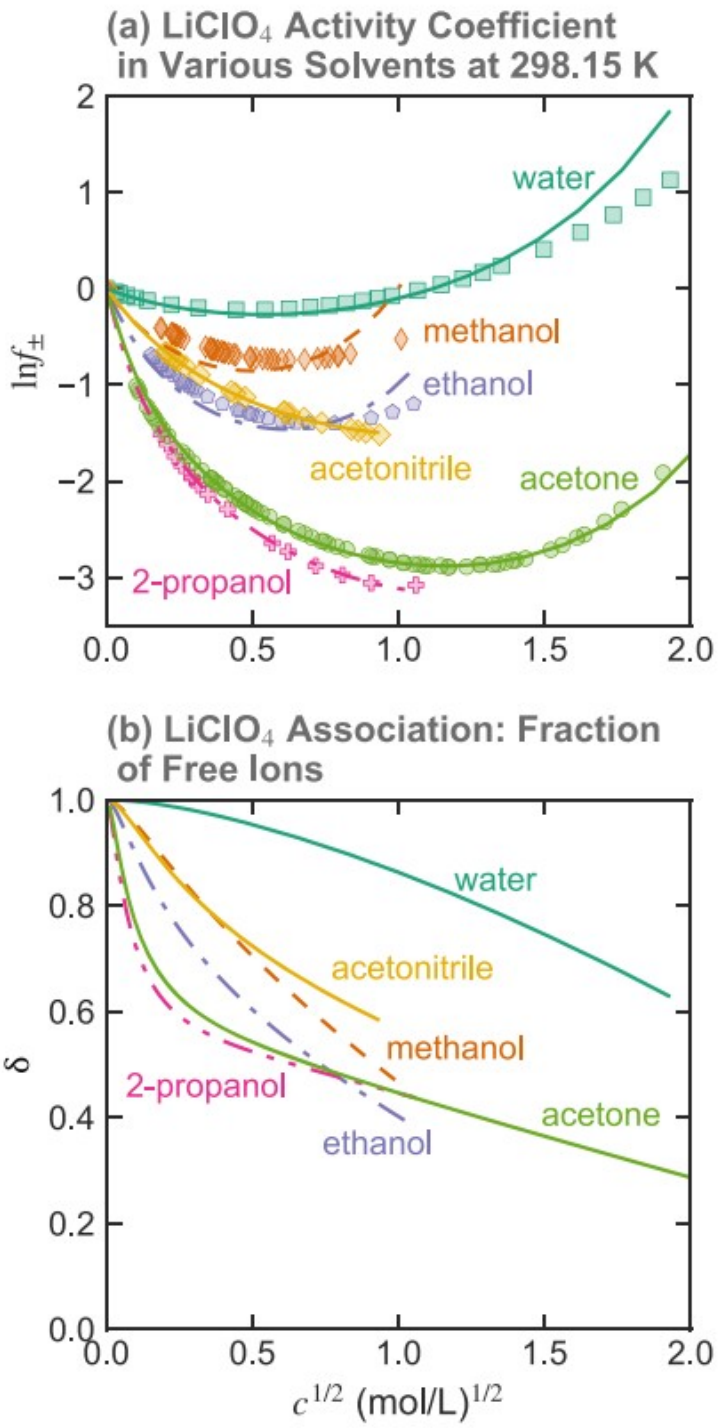

Figure 2. Measured (symbols) and calculated (lines) mean ion activity coefficient ln $f_{\pm}$ (a) and fraction of free ions δ (b) as a function of the square root of $LiClO_4$ concentration in water (squares and solid line, data from ref 48), methanol (thin diamonds and dashed line, data from ref 65), ethanol (pentagons and dot dashed line, data from ref 65), acetonitrile (thick diamonds and four-dotted dashed line, data from ref 60), acetone (circles and three-dot dashed line, data from ref 60), and 2-propanol (pluses and two-dot dashed line, data from ref 65) at 298.15 K.

Figure 2b demonstrates how ion association depends on concentration and solvent properties. Plotting the fraction of free $LiClO_4$ ions δ in water, methanol, ethanol, acetonitrile, acetone, and 2-propanol shows that δ decreases as concentration rises. In lower dielectric-constant solvents and for smaller σ, δ is concave to the concentration axis because of the larger association constant.

Table2 gives K, the calculated equilibrium constant for ion-pair formation. K calculated from eq 22 compares well with the equilibrium constant reported in the literature K^{lit} determined from conductance measurements.(57−60) Agreement between theory and experiment further supports the use of eq 22 and the fit σ's to calculate K.

Figure 3 shows the mean ionic activity coefficient for several lithium salts in water, $LiClO_4$, LiCl, LiBr, and LiI as a function of salt concentration. Agreement between theory and experiment for these four salts is good up to 2 molar with ARDs of 2.1, 1.4, 1.3, and 2.7. The insert in Figure 3 shows that theory is semiquantitative at higher concentrations due to changes in the solvation-shell size. Wu and Lee(19) and Simonin et al.(33,56) showed that incorporation of concentration-dependent ionic sizes and solution dielectric constant yields excellent fits to experiment up to saturation but such fits require numerous additional adjustable parameters.

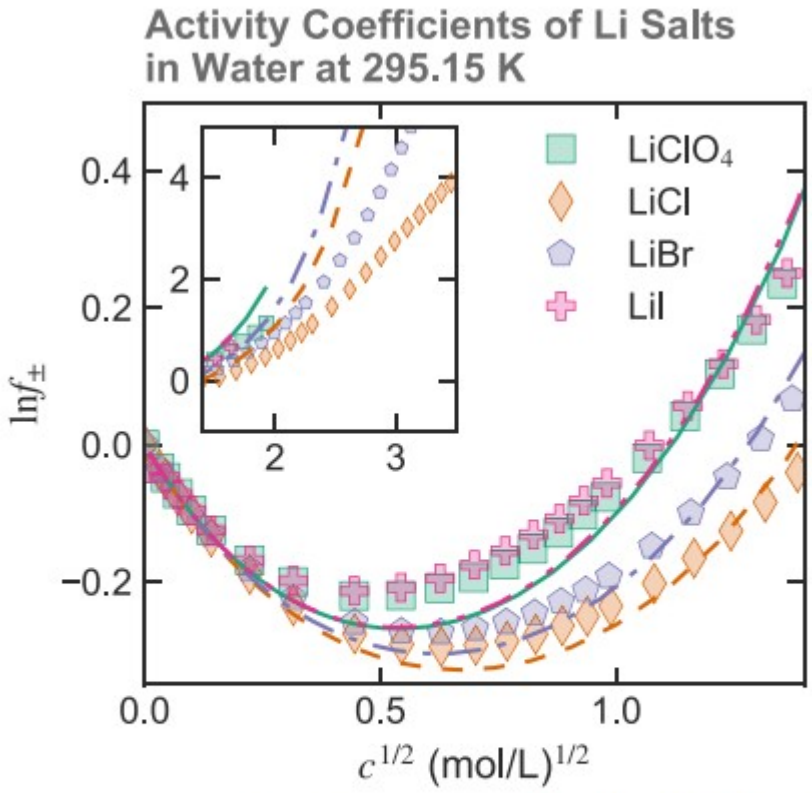

Figure 3. Measured (symbols, data from ref 48) and calculated (lines) mean ion activity coefficient ln $f_{\pm}$ in water as a function of the square root salt concentration for $LiClO_4$ (squares and solid line), LiCl (diamonds and dashed line), LiBr (pentagons and dot dashed line), and LiI (pluses and two-dot dashed line) at 298.15 K. Inset shows data over a higher range of salt concentrations.

For these lithium salts, there is little change in ω_s. Table3 gives fitted σ for these systems and the corresponding ω_s and *K*. The similarity of ω_s for different monatomic anions shows that the solvation structure is nearly independent of anion in these cases. Therefore, in a solvent, the size of the bare anion is responsible for different activity coefficients for different lithium salts. This result is consistent with previous research.(66) However, ω_s for $LiClO_4$ in water is slightly smaller than for monatomic anions (Table2). The difference in ω_s for monatomic and polyatomic anions is possibly because we model ions as spheres; that may not be a good approximation for polyatomic anions.

Table 3. Model Parameters for Three Lithium Salts in Water at 298.15 K

salt	σ [nm]	ω_s [a]	K [b]
LiCl	0.424	0.428	0.403
LiBr	0.438	0.425	0.389
LiI	0.464	0.430	0.365

[a] Equation 24 where $\sigma^x_{Cl^-}$ = 0.362 nm, $\sigma^x_{Br^-}$ = 0.392 nm, $\sigma^x_{I^-}$ = 0.440 nm.[62] [b] Equation 22.

Mixed-Solvent Electrolytes

In a mixed solvent, the solvent that has stronger attractive interactions with the ions preferentially solvates them. Wang and co-workers developed a theory to predict the extent of preferential solvation by accounting for permanent and induced dipole-ion interactions. The Supporting Information outlines this theory for calculating the volume fraction of solvent a at the surface of an isolated ion, φ_a^*, in a solvent with bulk volume fraction of ${}^a\varphi_a$. (21,22)

Figure 4 shows the volume fraction, calculated with the use of the theory outlined in the Supporting Information (lines), of solvent a at the surface of a Li^+ ion in a mixture of solvents a and b as a function of volume fraction of a in the bulk for two water/alcohol mixtures: water/ethanol (EtOH) and water/methanol (MeOH), and for two common lithium-ion-battery solvents: ethylene carbonate (EC)/dimethyl carbonate (DMC) and EC/ethyl methyl carbonate (EMC). As the fraction of solvent a in the bulk increases, the fraction at the ion's surface also increases but the relation is not linear. For the solvent that preferentially solvates the ion, the volume fraction at the surface of the ion is greater than that in the bulk.

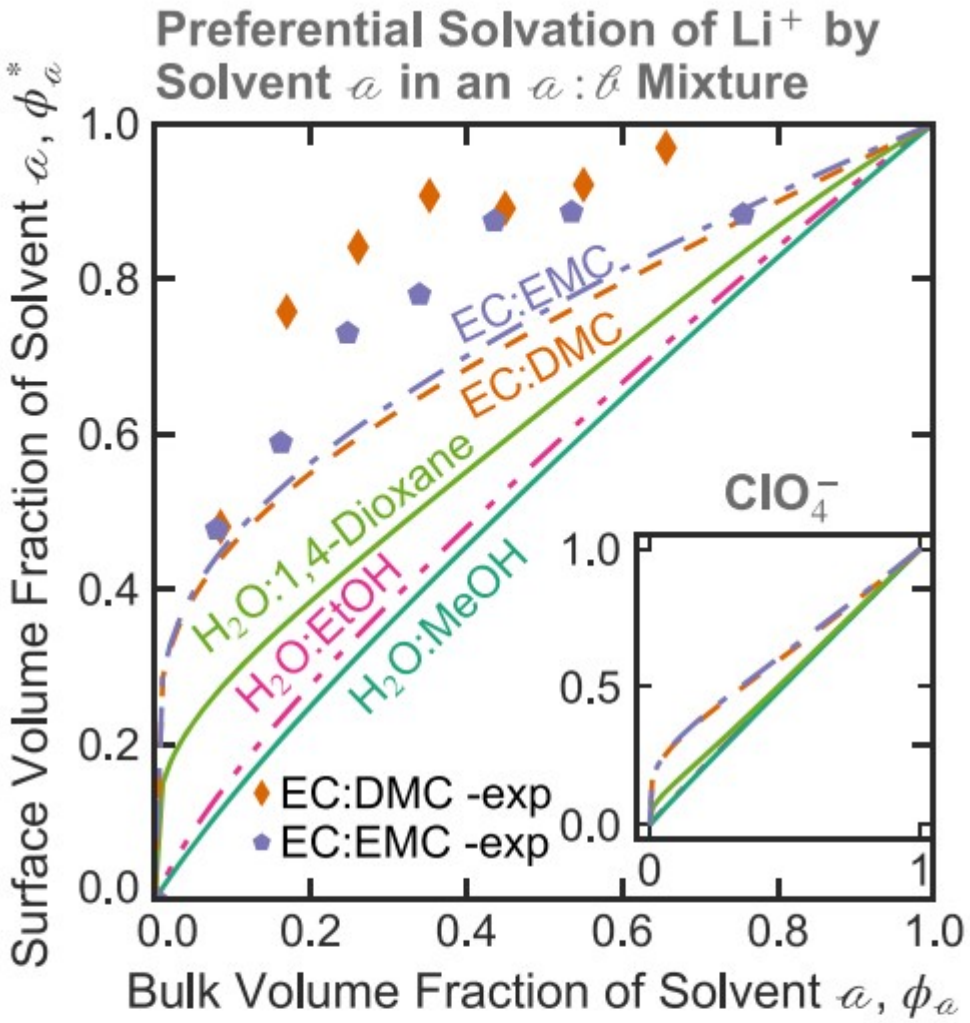

Figure 4. Measured (symbols, data from ref 67) and calculated from eq (SI1) (lines) volume fraction of solvent a at the surface φ_a^* of an isolated Li^+ ion as a function of bulk volume fraction of a φ_a in a/b mixtures of ethylene carbonate (EC)/ethyl methyl carbonate (EMC) (dot dashed line and pentagons), EC/dimethyl carbonate (DMC) (dashed line and diamonds), water (H_2O)/1,4-dioxane (three-dot dashed line), H_2O/ethanol (EtOH) (two-dot dashed line), and H_2O/methanol (MeOH) (solid line). Measurements are made using electrospray ionization mass spectrum techniques.[67] The inset shows predictions for ClO_4^- anion solvation in the same solvents as those in the main figure and denoted with the same line types.

For water/alcohol mixtures, the model shows that water's smaller size allows it to preferentially solvate the ions by packing tightly around the ion. In carbonate mixtures, EC preferentially solvates ions compared to DMC and EMC because of ECs smaller size and its larger dipole moment than those of

DMC or EMC. These predictions for carbonate mixtures are consistent with experiment. The solvation shell composition around Li^+ is known from electrospray-ionization mass spectrometry of a $LiPF_6$ electrolyte in EC/DMC and EC/EMC mixtures (data given as symbols in Figure 4).(67) Electrospray-ionization mass spectrometry does not fully capture in-solution conditions due to partial desolvation during the course of the measurement, causing some disagreement between experiment and theory.(67)

We calculate the preferential solvation of an anion to check that it is negligible. The inset in Figure 4 shows the calculated volume fraction of solvent a at the surface of a ClO_4^- anion as a function of bulk volume fraction of solvent a for the same solvent mixtures. The anion's large size decreases the electric field at the surface and, consequently, decreases preferential solvation, as shown in eq (SI1). The calculated insignificant preferential solvation of the anion is consistent with our assumption of negligible anion solvation that we invoked in our calculation of average salt diameter (eq 24).

Preferential Solvation and Activity Coefficients in a Solvent Mixture

A solvent mixture's preferential solvation of ions causes the average size of the solvation shell, ν^*_{ave}, to be a function of solvent composition at the ion surface

$$\nu^*_{ave} = \sum_t \varphi_t^* \nu_t = \sum_t \varphi_t^* \frac{\pi}{6} \sigma_t^3 \omega_t^3 \quad (26)$$

where ω_t is the sphericity factor of solvent t. Using eq 26, we incorporate preferential solvation into BiMSA by modifying eqs 24 where we use an effective solvent diameter for the solvated cation

$$\sigma_+ = \frac{\left(\sigma_+^3 + \sigma_-^3 + 3\left(\frac{6}{\pi}\nu^*_{ave}\omega_{ave}\right)^{1/3}\right)}{2} = \frac{\left(\sigma_+^3 + \sigma_-^3 + 3\left(\sum_t \varphi_t^* \sigma_t^3 \omega_t^3\right)^{1/3}\right)}{2} \quad (27)$$

This solvated diameter provides a molecular basis for calculating activity coefficient $f_\pm$ in a mixed solvent with parameter ω_t for each solvent t in the mixture.

Figure 5 shows calculated (lines) and measured (symbols) mean ion activity coefficients for LiCl in mixtures of H_2O/MeOH (a),(68,69) /EtOH (b),(70,71)/acetonitrile (c),(68) and /1,4-dioxane(68) at 298.15 K with varying H_2O bulk solvent compositions. We put ω_t into eq 27 and in turn, in eq 16, where φ_t^* is given by the solution of eqs SI1–SI3. Table4 gives ε_r and salt-free solvent mixture density ρ_s for different solvent compositions determined by measurements.(68−72) To calculate ω_t of a nonaqueous component of a mixed-solvent electrolyte, we fit σ to the measured mean ion activity coefficient for LiCl in that solvent and use eq 27. (If salt-in-single-solvent activity coefficients are not available, we use the solvent mixture that is richest in that solvent.) Table4 gives ω_t for nonaquous solvents and Table3 gives $\omega_{H2}O$ for LiCl. Upon specifying ω_t for each solvent with LiCl, ω_t is independent of salt concentration and composition ratio of the solvent

mixture. For nonaqueous solvents, ω_t values for LiCl given in Table4 are different from those for $LiClO_4$ given in Table2. For solvent mixtures, because experimental data are not available, we assume that the density of the solution does not significantly change from those of the salt-free solvent mixture such that $\rho_s^0/\rho_s = 1$ in eq 3.

Table 4. Properties of Salt-Free Solvent Mixtures. ε_r Is the Dielectric Constant and d_s^0 is the Density of the Salt-Free Solvent Mixture at 298.15 K

	weight fraction H_2O	ε_r	d_s^0 [g cm^{-3}]
H_2O/MeOH[68,69,72] $\omega_{MeOH} = 0.54$	0.8	70.0	0.968
	0.6	60.9	0.937
	0.4	51.7	0.898
	0.2	42.6	0.851
	0.0	32.6	0.792
H_2O/EtOH[70−72] $\omega_{EtOH} = 0.53$	0.8	67.0	0.966
	0.6	55.0	0.932
	0.4	43.4	0.887
	0.2	32.8	0.839
	0.0	24.9	0.789
H_2O/acetonitrile[68] $\omega_{acetonitrile} = 0.40$	0.9	75.0	0.981
	0.8	70.5	0.961
	0.7	65.5	0.939
	0.6	60.4	0.916
H_2O/1,4-dioxane[68] $\omega_{dioxane} = 0.65$	0.9	70.3	1.01
	0.8	61.9	1.01
	0.6	44.5	1.03
	0.4	27.2	1.04

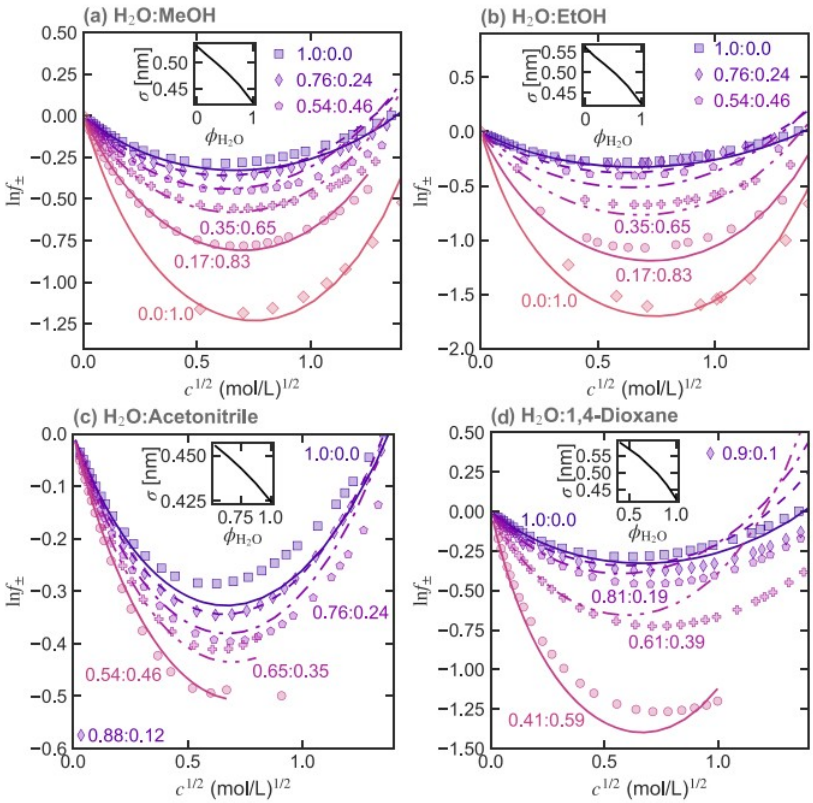

Figure 5. Measured (symbols) and calculated (lines) ln $f_{\pm}$ for LiCl in mixtures of water/methanol (a, data from refs 68 and 69), water/ethanol (b, data from refs 70 and 71), water/acetonitrile (c, data from ref 68), and water/1,4-dioxane (d, data from ref 68) for various volume fractions of each solvent (noted in the figure) at 298.15 K. The insets show ion diameter σ as a function of bulk solvent water volume fraction, ϕ_{H_2O}.

The insets in Figure 5 show calculated diameters σ as a function of solvent–mixture composition where $\phi_{H2}O$ is the bulk volume fraction of water. Theory agrees well with experiment for H_2O/MeOH, H_2O/EtOH, and H_2O/acetonitrile mixtures but not for H_2O/dioxane. The poor agreement for dioxane illustrates a limitation of the solvation theory (eq SI1) for large-molecule solvents where molecular geometry is important. The theoretical calculations discussed here assume that the ion diameter does not change with ion concentration. There is no obvious way to relax that assumption without introducing additional adjustable parameters.

The model shows that at low salt concentrations, increasing the amount of low-dielectric-constant solvent in the mixture decreases the activity coefficient. This result follows from long-range, favorable electrostatic interactions that increase with decreasing dielectric constant. However, at higher salt concentrations, repulsive steric interactions increase, raising the salt activity coefficient. This steric effect is more pronounced as water is replaced by larger solvent molecules that create larger solvation shells around Li^+. The insets in Figure 5 show that the distance of closest approach between the ions is not a linear function of bulk solvent composition, illustrating the effect of preferential solvation on electrolyte activity in mixed solvents.

Implications for Transport

An important implication of mixed-solvent electrolyte thermodynamic properties in renewable energy applications is their impact on transport properties.(73) In an ideal solution, species diffuse down their concentration gradients at a rate proportional to their diffusivity. However, for nonideal mixtures, ions diffuse down their chemical-potential gradients. Consequently, the diffusivity is modified in solutions to account for nonideality by multiplying it by the thermodynamic factor(74)

Figure 6 shows the calculated thermodynamic factor with $f_{\pm}$ from eq 16 for $LiClO_4$ in water (solid line), acetonitrile (double dot-dashed line), acetone (dot-dashed line), and 2-propanol (dashed line). At infinite dilution, the thermodynamic factor is unity. At low salt concentrations, the thermodynamic factor decreases with rising salt concentration. The extent of this initial drop increases for solvents with lower dielectric constants. At higher salt concentrations, the thermodynamic factor rises with increasing salt concentration.

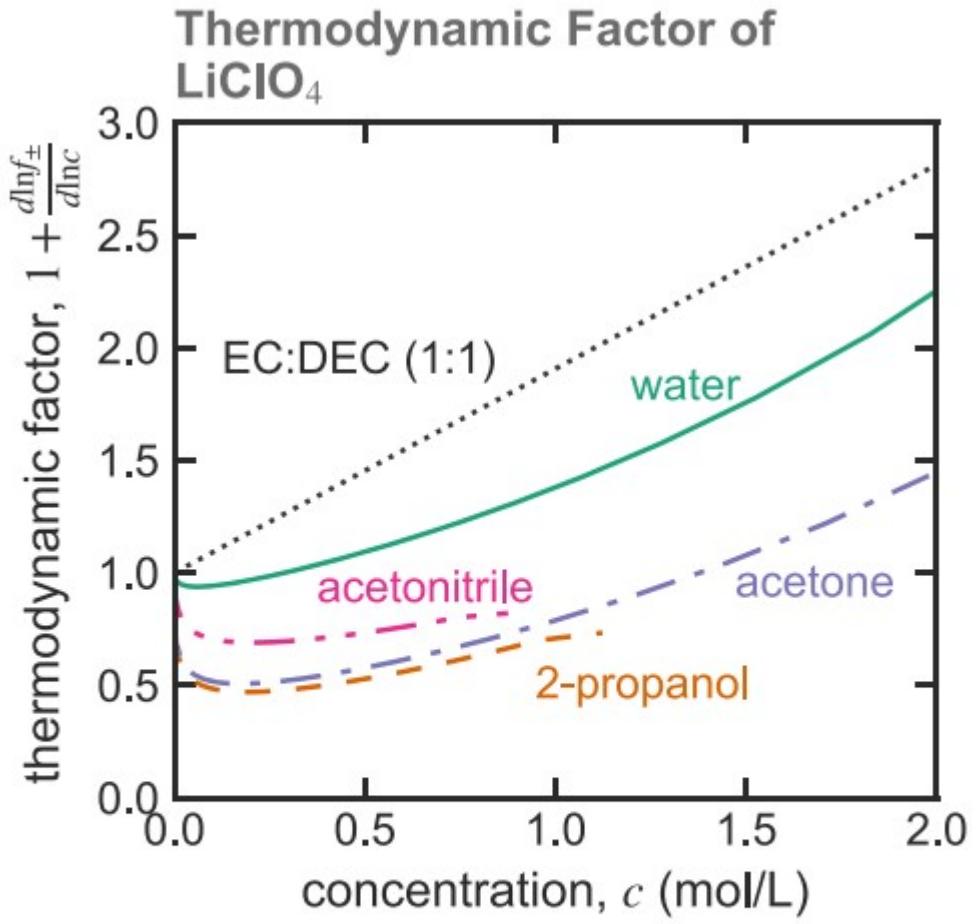

Figure 6. Calculated thermodynamic factor for $LiClO_4$ in water (solid line), acetonitrile (double dot-dashed line), acetone (dot-dashed line), and 2-propanol (dashed line) at 298.15 K. The dotted line shows the experimental thermodynamic factor of $LiClO_4$ in a 1:1 (w:w) mixture of ED/DEC (data from ref 5).

Landesfeind et al. measured the thermodynamic factor for $LiClO_4$ in a 1:1 (w:w) mixture of EC/DEC (diethyl carbonate) using an electrochemical method,(5) shown by the dotted line in Figure 6. This last thermodynamic factor deviates significantly from those for the other electrolytes even though the solvent mixture has a dielectric constant ($\varepsilon_r = 35$) similar to those for the other aprotic solvents. This discrepancy may be due to the large solvent molecule size that increases σ.

Conclusions

This work presents a theory for activity coefficients of lithium salts in aqueous and nonaqueous single and mixed solvents. The BiMSA theory gives electrolyte activity coefficients. This theory considers long-range electrostatic and short-range hard-sphere interactions as well as ion pairing. BiMSA theory shows good agreement with measured salt activity coefficients

in aqueous and nonaqueous electrolytes with a single adjustable parameter (the distance of closest approach between ions, σ), for each salt in each solvent. The fitted ion diameters are within the expected range.

The extension to mixed-solvent electrolytes is based on Wang's theory for preferential ion solvation that changes σ as a function of solvent composition. This theory predicts the mean ion activity coefficients of salts in solvent mixtures using only single-solvent fitting parameters.

At present, this work is limited to strong 1−1 salts. Extension to multivalent salts is under investigation. This work illustrates how microscopic molecular physics can describe macroscopic electrolyte activity coefficients over a range of salt concentrations and solvent types and for mixtures using minimal adjustable parameters.

Acknowledgments

This work was funded in part by a National Science Foundation Graduate Research Fellowship under Grant DGE 1106400. For partial financial support, the authors thank Prof. C.C. Chen of Texas Tech University in Lubbock, Texas.

References

1

Delacourt, C.; Ridgway, P. L.; Kerr, J. B.; Newman, J. Design of an Electrochemical Cell Making Syngas (CO+H2) from CO2 and H2O Reduction at Room Temperature. *J. Electrochem. Soc.* 2008, *155* (1), B42– B49, DOI: 10.1149/1.2801871

2

Singh, M. R.; Bell, A. T. Design of an artificial photosynthetic system for production of alcohols in high concentration from CO2. *Energy Environ. Sci.* 2016, *9* (1), 193– 199, DOI: 10.1039/C5EE02783G

3

Perry, M. L.; Weber, A. Z. Advanced Redox-Flow Batteries: A Perspective. *J. Electrochem. Soc.* 2016, *163* (1), A5064– A5067, DOI: 10.1149/2.0101601jes

4

Singh, M. R.; Kwon, Y.; Lum, Y.; Ager, J. W.; Bell, A. T. Hydrolysis of Electrolyte Cations Enhances the Electrochemical Reduction of CO2 over Ag and Cu. *J. Am. Chem. Soc.* 2016, *138* (39), 13006– 13012, DOI: 10.1021/jacs.6b07612

5

Landesfeind, J.; Ehrl, A.; Graf, M.; Wall, W. A.; Gasteiger, H. A. Direct Electrochemical Determination of Thermodynamic Factors in Aprotic Binary

Electrolytes. *J. Electrochem. Soc.* 2016, *163* (7), A1254– A1264, DOI: 10.1149/2.0651607jes

6

Newman, J.; Thomas-Alyea, K. E. *Electrochemical Systems*; John Wiley & Sons, 2004; p 674.

7

Robinson, R. A.; Stokes, R. H. *Electrolyte solutions*; Courier Corporation, 2002.

8

Kontogeorgis, G. M.; Maribo-Mogensen, B.; Thomsen, K. The Debye-Hückel theory and its importance in modeling electrolyte solutions. *Fluid Phase Equilib.* 2018, *462*, 130– 152, DOI: 10.1016/j.fluid.2018.01.004

9

Barthel, J.; Krienke, H.; Holovko, M.; Kapko, V.; Protsykevich, I. The application of the associative mean spherical approximation in the theory of nonaqueous electrolyte solutions. *Condens. Matter Phys.* 2000, *3* (3), 657, DOI: 10.5488/CMP.3.3.657

10

Held, C.; Prinz, A.; Wallmeyer, V.; Sadowski, G. Measuring and modeling alcohol/salt systems. *Chem. Eng. Sci.* 2012, *68* (1), 328– 339, DOI: 10.1016/j.ces.2011.09.040

11

Zerres, H.; Prausnitz, J. M. Thermodynamics of phase equilibria in aqueous-organic systems with salt. *AIChE J.* 1994, *40* (4), 676– 691, DOI: 10.1002/aic.690400411

12

Ahmed, S.; Ferrando, N.; Hemptinne, J.-C. d.; Simonin, J.-P.; Bernard, O.; Baudouin, O. Modeling of mixed-solvent electrolyte systems. *Fluid Phase Equilib.* 2018, *459*, 138– 157, DOI: 10.1016/j.fluid.2017.12.002

13

Xin, N.; Sun, Y.; Radke, C. J.; Prausnitz, J. M. Osmotic and activity coefficients for five lithium salts in three non–aqueous solvents. *J. Chem. Thermodyn.* 2019, *132*, 83– 92, DOI: 10.1016/j.jct.2018.12.016

14

Chapman, W. G.; Gubbins, K. E.; Jackson, G.; Radosz, M. SAFT: Equation-of-state solution model for associating fluids. *Fluid Phase Equilib.* 1989, *52*, 31–38, DOI: 10.1016/0378-3812(89)80308-5

15

Economou, I. G.; Donohue, M. D. Equation of state with multiple associating sites for water and water-hydrocarbon mixtures. *Ind. Eng. Chem. Res.* 1992, *31* (10), 2388– 2394, DOI: 10.1021/ie00010a019

16

Pitzer, K. S.; Mayorga, G. Thermodynamics of Electrolytes: II. Activity and Osmotic Coefficients for Strong Electrolytes with One or Both Ions Univalent. In *Molecular Structure and Statistical Thermodynamics*; World Scientific, 1993, pp 396– 404.

17

Pitzer, K. S. *Activity Coefficients in Electrolyte Solutions*; CRC Press, 2018.

18

Prausnitz, J. M., Lichtenthaler, R. N., de Azevedo, E. G. *Molecular thermodynamics of fluid-phase equilibria*; Pearson Education, 1998.

19

Wu, R.-S.; Lee, L. L. Vapor-liquid equilibria of mixed-solvent electrolyte solutions: ion-size effects based on the MSA theory. *Fluid Phase Equilib.* 1992, *78*, 1– 24, DOI: 10.1016/0378-3812(92)87026-J

20

Marcus, Y. Preferential solvation of ions in mixed solvents. Part 2.—The solvent composition near the ion. *J. Chem. Soc., Faraday Trans. 1* 1988, *84* (5), 1465– 1473, DOI: 10.1039/f19888401465

21

Nakamura, I.; Shi, A.-C.; Wang, Z.-G. Ion Solvation in Liquid Mixtures: Effects of Solvent Reorganization. *Phys. Rev. Lett.* 2012, *109* (25), 257802, DOI: 10.1103/PhysRevLett.109.257802

22

Zhuang, B.; Wang, Z.-G. Molecular-Based Theory for Electron-Transfer Reorganization Energy in Solvent Mixtures. *J. Phys. Chem. B* 2016, *120* (26), 6373– 6382, DOI: 10.1021/acs.jpcb.6b03295

23

Salimi, H. R.; Taghikhani, V.; Ghotbi, C. Application of the GV-MSA model to the electrolyte solutions containing mixed salts and mixed solvents. *Fluid Phase Equilib.* 2005, *231* (1), 67– 76, DOI: 10.1016/j.fluid.2004.12.015

24

Maribo-Mogensen, B.; Thomsen, K.; Kontogeorgis, G. M. An electrolyte CPA equation of state for mixed solvent electrolytes. *AIChE J.* 2015, *61* (9), 2933– 2950, DOI: 10.1002/aic.14829

25

Chen, C. C.; Song, Y. Generalized electrolyte-NRTL model for mixed-solvent electrolyte systems. *AIChE J.* 2004, *50* (8), 1928– 1941, DOI: 10.1002/aic.10151

26

Ye, S.; Xans, P.; Lagourette, B. Modification of the Pitzer model to calculate the mean activity coefficients of electrolytes in a water-alcohol mixed solvent solution. *J. Solution Chem.* 1994, *23* (12), 1301– 1315, DOI: 10.1007/BF00974183

27

Das, G.; dos Ramos, M. C.; McCabe, C. Predicting the thermodynamic properties of experimental mixed-solvent electrolyte systems using the SAFT-VR+DE equation of state. *Fluid Phase Equilib.* 2018, *460*, 105– 118, DOI: 10.1016/j.fluid.2017.11.017

28

Gupta, A. R. Thermodynamics of electrolytes in mixed solvents. Application of Pitzer's thermodynamic equations to activity coefficients of 1:1 electrolytes in methanol-water mixtures. *J. Phys. Chem.* 1979, *83* (23), 2986– 2990, DOI: 10.1021/j100486a010

29

Barthel, J. M.; Krienke, H.; Kunz, W. *Physical chemistry of electrolyte solutions: modern aspects*; Springer Science & Business Media, 1998; Vol. 5.

30

Lee, L. L. *Molecular thermodynamics of electrolyte solutions*; World Scientific: Singapore; Hackensack, NJ, 2008.

31

Blum, L. Mean spherical model for asymmetric electrolytes. *Mol. Phys.* 1975, *30* (5), 1529– 1535, DOI: 10.1080/00268977500103051

32

Bernard, O.; Blum, L. Binding mean spherical approximation for pairing ions: An exponential approximation and thermodynamics. *J. Chem. Phys.* 1996, *104* (12), 4746– 4754, DOI: 10.1063/1.471168

33

Simonin, J.-P.; Bernard, O.; Blum, L. Real Ionic Solutions in the Mean Spherical Approximation. 3. Osmotic and Activity Coefficients for Associating Electrolytes in the Primitive Model. *J. Phys. Chem. B* 1998, *102* (22), 4411– 4417, DOI: 10.1021/jp9732423

34

Haynes, C. A.; Newman, J. On converting from the McMillan-Mayer framework I. Single-solvent system. *Fluid Phase Equilib.* 1998, *145* (2), 255– 268, DOI: 10.1016/S0378-3812(97)00335-X

35

Lee, L. L. Thermodynamic consistency and reference scale conversion in multisolvent electrolyte solutions. *J. Mol. Liq.* 2000, *87* (2), 129– 147, DOI: 10.1016/S0167-7322(00)00117-3

36

Blum, L. Primitive Electrolytes in the Mean Spherical Approximation. In *Theoretical Chemistry*; Eyring, H.; Henderson, D., Eds.; Academic Press, 1980; pp 1– 66.

37

Cabezas, H.; O'Connell, J. P. Some uses and misuses of thermodynamic models for dilute liquid solutions. *Ind. Eng. Chem. Res.* 1993, *32* (11), 2892– 2904, DOI: 10.1021/ie00023a063

38

Ornstein, L. S. Accidental deviations of density and opalescence at the critical point of a single substance. *Proc. Akad. Sci.* 1914, *17*, 793

39

Gores, H. J.; Barthel, J.; Zugmann, S.; Moosbauer, D.; Amereller, M.; Hartl, R.; Maurer, A. Liquid Nonaqueous Electrolytes. In *Handbook of Battery Materials*; Wiley-VCH Verlag GmbH & Co. KGaA, 2011; pp 525– 626.

40

Blum, L.; Høye, J. Mean spherical model for asymmetric electrolytes. 2. Thermodynamic properties and the pair correlation function. *J. Phys. Chem.* 1977, *81* (13), 1311– 1316, DOI: 10.1021/j100528a019

41

Harvey, A. H.; Copeman, T. W.; Prausnitz, J. M. Explicit approximations to the mean spherical approximation for electrolyte systems with unequal ion sizes. *J. Phys. Chem.* 1988, *92* (22), 6432– 6436, DOI: 10.1021/j100333a047

42

Wertheim, M. S. Fluids with highly directional attractive forces. I. Statistical thermodynamics. *J. Stat. Phys.* 1984, *35* (1), 19– 34, DOI: 10.1007/BF01017362

43

Simonin, J.-P.; Bernard, O.; Blum, L. Ionic Solutions in the Binding Mean Spherical Approximation: Thermodynamic Properties of Mixtures of

Associating Electrolytes. *J. Phys. Chem. B* 1999, *103* (4), 699– 704, DOI: 10.1021/jp9833000

44

Stokes, R. H.; Robinson, R. A. Ionic Hydration and Activity in Electrolyte Solutions. *J. Am. Chem. Soc.* 1948, *70* (5), 1870– 1878, DOI: 10.1021/ja01185a065

45

Krienke, H.; Barthel, J.; Holovko, M.; Protsykevich, I.; Kalyushnyi, Y. Osmotic and activity coefficients of strongly associated electrolytes over large concentration ranges from chemical model calculations. *J. Mol. Liq.* 2000, *87* (2), 191– 216, DOI: 10.1016/S0167-7322(00)00121-5

46

Ebeling, W. Zur Theorie der Bjerrumschen Ionenassoziation in Elektrolyten. *Z. Phys. Chem.* 1968, *238O*, 400, DOI: 10.1515/zpch-1968-23847

47

Bockris, J. O. M.; Conway, B. E.; White, R. E. *Modern aspects of electrochemistry*; Springer Science & Business Media, 2012; Vol. 22.

48

CRC handbook of chemistry and physics; CRC Press: Cleveland, OH, 1978.

49

Nelson, R. D.; Lide, D. R.; Maryott, A. A.; Standards, U. S. N. B. o. *Selected Values of Electric Dipole Moments for Molecules in the Gas Phase*; U.S. National Bureau of Standards, 1967.

50

Seward, R. P.; Vieira, E. C. The Dielectric Constants of Ethylene Carbonate and of Solutions of Ethylene Carbonate in Water, Methanol, Benzene and Propylene Carbonate. *J. Phys. Chem.* 1958, *62* (1), 127– 128, DOI: 10.1021/j150559a041

51

Arai, J. A novel non-flammable electrolyte containing methyl nonafluorobutyl ether for lithium secondary batteries. *J. Appl. Electrochem.* 2002, *32* (10), 1071– 1079, DOI: 10.1023/A:1021231514663

52

Payne, R.; Theodorou, I. E. Dielectric properties and relaxation in ethylene carbonate and propylene carbonate. *J. Phys. Chem.* 1972, *76* (20), 2892– 2900, DOI: 10.1021/j100664a019

53

Bosque, R.; Sales, J. Polarizabilities of Solvents from the Chemical Composition. *J. Chem. Inf. Comput. Sci.* 2002, *42* (5), 1154– 1163, DOI: 10.1021/ci025528x

54

Iglesias-Otero, M. A.; Troncoso, J.; Carballo, E.; Romaní, L. Density and Refractive Index for Binary Systems of the Ionic Liquid [Bmim][BF4] with Methanol, 1,3-Dichloropropane, and Dimethyl Carbonate. *J. Solution Chem.* 2007, *36* (10), 1219, DOI: 10.1007/s10953-007-9186-6

55

Krienke, H.; Barthel, J. MSA models of ion association in electrolyte solutions. *Z. Phys. Chem.* 1998, *204* (1–2), 71– 83, DOI: 10.1524/zpch.1998.204.Part_1_2.071

56

Simonin, J.-P.; Bernard, O. Organic electrolyte solutions: Modeling of deviations from ideality within the binding mean spherical approximation. *Fluid Phase Equilib.* 2018, *468*, 58– 69, DOI: 10.1016/j.fluid.2017.11.018

57

Barthel, J., Neueder, R. *Electrolyte Data Collection: Conductivities, transference numbers, limiting ionic conductivities*; Dechema, 1993; Vol. 1.

58

Schmelzer, N.; Einfeldt, J.; Grigo, M. Measurements of the electrolyte conductivity of alkali-metal perchlorates and LiNO3 in acetone at 25 °C. *J. Chem. Soc., Faraday Trans. 1* 1988, *84* (4), 931– 939, DOI: 10.1039/f19888400931

59

Barthel, J.; Neueder, R.; Schroder, P. Electrolyte Data Collection: Part 1c: Conductivities, Tranference Numbers, and Limiting Ionic Conductivities of Solutions of Aprotic, Protophobic Solvents: I; Nitriles. *DECHEMA, Deutsche Gesellschaft fur Chemisches Apparatewese, Chemische* 1997, *101*, 151, DOI: 10.1002/bbpc.19971010125

60

Barthel, J.; Neueder, R.; Poepke, H.; Wittmann, H. Osmotic Coefficients and Activity Coefficients of Nonaqueous Electrolyte Solutions. Part 2. Lithium Perchlorate in the Aprotic Solvents Acetone, Acetonitrile, Dimethoxyethane, and Dimethylcarbonate. *J. Solution Chem.* 1999, *28* (5), 489– 503, DOI: 10.1023/A:1022674613995

61

Shannon, R. Revised effective ionic radii and systematic studies of interatomic distances in halides and chalcogenides. *Acta Crystallogr., Sect.*

A: Cryst. Phys., Diffr., Theor. Gen. Crystallogr. 1976, *32* (5), 751– 767, DOI: 10.1107/S0567739476001551

62

Jenkins, H.; Thakur, K. Reappraisal of thermochemical radii for complex ions. *J. Chem. Educ.* 1979, *56* (9), 576, DOI: 10.1021/ed056p576

63

Bockris, J. O. M.; Reddy, A. K. N.; Gamboa-Aldeco, M. E. *Modern electrochemistry*, 2nd ed.; Plenum Press: New York, 1998.

64

Held, C.; Sadowski, G. Modeling aqueous electrolyte solutions. Part 2. Weak electrolytes. *Fluid Phase Equilib.* 2009, *279* (2), 141– 148, DOI: 10.1016/j.fluid.2009.02.015

65

Barthel, J.; Neueder, R.; Poepke, H.; Wittmann, H. Osmotic and Activity Coefficients of Nonaqueous Electrolyte Solutions. 1. Lithium Perchlorate in the Protic Solvents Methanol, Ethanol, and 2-Propanol. *J. Solution Chem.* 1998, *27* (12), 1055– 1066, DOI: 10.1023/A:1022637316064

66

Held, C.; Cameretti, L. F.; Sadowski, G. Modeling aqueous electrolyte solutions: Part 1. Fully dissociated electrolytes. *Fluid Phase Equilib.* 2008, *270* (1), 87– 96, DOI: 10.1016/j.fluid.2008.06.010

67

von Cresce, A.; Xu, K. Preferential Solvation of Li+ Directs Formation of Interphase on Graphitic Anode. *Electrochem. Solid-State Lett.* 2011, *14* (10), A154– A156, DOI: 10.1149/1.3615828

68

Mussini, P. R.; Mussini, T.; Sala, B. Thermodynamics of the cell { Li- Amalgam | LiX (m)| AgX | Ag }(X = Cl,Br) and medium effects upon LiX in (acetonitrile + water), (1,4-dioxane + water), and (methanol + water) solvent mixtures with related solvation parameters. *J. Chem. Thermodyn.* 2000, *32* (5), 597– 616, DOI: 10.1006/jcht.1999.0622

69

Safarov, J. T. Study of thermodynamic properties of binary solutions of lithium bromide or lithium chloride with methanol. *Fluid Phase Equilib.* 2005, *236* (1), 87– 95, DOI: 10.1016/j.fluid.2005.07.002

70

Safarov, J. T. Vapor pressures of lithium bromide or lithium chloride and ethanol solutions. *Fluid Phase Equilib.* 2006, *243* (1), 38– 44, DOI: 10.1016/j.fluid.2006.02.012

71

Hernández-Luis, F.; Galleguillos, H. R.; Graber, T. A.; Taboada, M. E. Activity Coefficients of LiCl in Ethanol-Water Mixtures at 298.15 K. *Ind. Eng. Chem. Res.* 2008, *47* (6), 2056– 2062, DOI: 10.1021/ie070704i

72

Hernández-Luis, F.; Vázquez, M. V.; Esteso, M. A. Activity coefficients for NaF in methanol-water and ethanol-water mixtures at 25°C. *J. Mol. Liq.* 2003, *108* (1), 283– 301, DOI: 10.1016/S0167-7322(03)00187-9

73

Shah, D. B.; Nguyen, H. Q.; Grundy, L. S.; Olson, K. R.; Mecham, S. J.; DeSimone, J. M.; Balsara, N. P. Difference between approximate and rigorously measured transference numbers in fluorinated electrolytes. *Phys. Chem. Chem. Phys.* 2019, *21* (15), 7857– 7866, DOI: 10.1039/C9CP00216B

74

Newman, J.; Thomas-Alyea, K. E. *Electrochemical systems*; John Wiley & Sons, 2012.